Inorg. Chem. **2005**, *44*, 1319–1331

Redox Control of Light-Induced Charge Separation in a Transition Metal Cluster: Photochemistry of a Methyl Viologen-Substituted $[Os_3(CO)_{10}(\alpha\text{-diimine})]$ Cluster

Frank W. Vergeer,[†,‡] Cornelis J. Kleverlaan,[§] Pavel Matousek,[||] Michael Towrie,[||] Derk J. Stufkens,[#] and František Hartl*,[†]

Institute of Molecular Chemistry, Universiteit van Amsterdam, Nieuwe Achtergracht 166, 1018 WV Amsterdam, The Netherlands, Academic Center for Dentistry Amsterdam, Louwesweg 1, 1066 EA Amsterdam, The Netherlands, and Central Laser Facility, CCLRC Rutherford Appleton Laboratory, Chilton, Didcot, Oxfordshire, U.K. OX11 0QX

Received June 21, 2004

(Sub)picosecond transient absorption (TA) and time-resolved infrared (TRIR) spectra of the cluster $[Os_3(CO)_{10}$-(AcPy-MV)$]^{2+}$ (the dication AcPy-MV = AcPy-MV^{2+} = [2-pyridylacetimine-*N*-(2-(1′-methyl-4,4′-bipyridine-1,1′-diium-1-yl)ethyl)]$(PF_6)_2$) (**1**$^{2+}$) reveal that photoinduced electron transfer to the electron-accepting 4,4′-bipyridine-1,1′-diium (MV^{2+}) moiety competes with the fast relaxation of the initially populated $\sigma\pi^*$ excited state of the cluster to the ground state and/or cleavage of an Os–Os bond. The TA spectra of cluster **1**$^{2+}$ in *acetone*, obtained by irradiation into its lowest-energy absorption band, show the characteristic absorptions of the one-electron-reduced $MV^{\bullet+}$ unit at 400 and 615 nm, in accordance with population of a charge-separated (CS) state in which a cluster-core electron has been transferred to the lowest π^* orbital of the remote MV^{2+} unit. This assignment is confirmed by picosecond TRIR spectra that show a large shift of the pilot highest-frequency ν(CO) band of **1**$^{2+}$ by ca. +40 cm^{-1}, reflecting the photooxidation of the cluster core. The CS state is populated via fast (4.2×10^{11} s^{-1}) and efficient (88%) oxidative quenching of the optically populated $\sigma\pi^*$ excited state and decays biexponentially with lifetimes of 38 and 166 ps (1.2:1 ratio) with a complete regeneration of the parent cluster. About 12% of the cluster molecules in the $\sigma\pi^*$ excited state form long-lived open-core biradicals. In strongly coordinating *acetonitrile*, however, the cluster core-to-MV^{2+} electron transfer in cluster **1**$^{2+}$ results in the irreversible formation of secondary photoproducts with a photooxidized cluster core. The photochemical behavior of the $[Os_3(CO)_{10}(\alpha\text{-diimine-MV})]^{2+}$ (donor–acceptor) dyad can be controlled by an externally applied electronic bias. Electrochemical one-electron reduction of the MV^{2+} moiety prior to the irradiation reduces its electron-accepting character to such an extent that the photoinduced electron transfer to $MV^{\bullet+}$ is no longer feasible. Instead, the irradiation of reduced cluster **1**$^{\bullet+}$ results in the reversible formation of an open-core zwitterion, the ultimate photoproduct also observed upon irradiation of related nonsubstituted clusters $[Os_3(CO)_{10}(\alpha\text{-diimine})]$ in strongly coordinating solvents such as acetonitrile.

Introduction

The control of electron-transfer reactions through specific (non)covalent interactions is a general phenomenon in many biological processes, such as respiration and photosynthesis. Aimed at understanding the fundamental principles underlying the often remarkable quantum efficiency of these reactions, considerable research efforts have been devoted to the design of supramolecular systems capable of mimicking, at the molecular level, the functions normally performed by a natural system. As examples may serve light-harvesting antenna systems,[1−6] artificial reaction centers,[7−11] or molecular switches.[12]

* Author to whom correspondence should be addressed. E-mail: f.hartl@uva.nl.
[†] Universiteit van Amsterdam.
[‡] Current address: Physikalisches Institut, University of Münster, Wilhelm Klemm-Strasse 10, D-48149 Münster, Germany.
[§] Academic Center for Dentistry, Amsterdam.
[||] CCLRC Rutherford Appleton Laboratory.
[#] Deceased.

(1) Kobuke, Y.; Ogawa, K. *Bull. Chem. Soc. Jpn.* **2003**, *76*, 689−708.
(2) Prathapan, S.; Johnson, T. E.; Lindsey, J. S. *J. Am. Chem. Soc.* **1993**, *115*, 7519−7520.
(3) Hsiao, J.-S.; Krueger, B. P.; Wagner, R. W.; Johnson, T. E.; Delaney, J. K.; Mauzerall, D. C.; Fleming, G. R.; Lindsey, J. S.; Bocian, D. F.; Donohoe, R. J. *J. Am. Chem. Soc.* **1996**, *118*, 11181−11193.

10.1021/ic049191n CCC: $30.25
Published on Web 02/15/2005

Current attention is also paid to molecular-scale electronic and photonic devices, the latter using absorbed light as the energy source.[13] Their function relies on energy- or electron-transfer processes taking place between the different components of the supramolecular assembly. Critical for their effective functioning is the competition between productive and nonproductive electron-transfer processes, where the nonproductive one usually concerns fast back electron transfer prior to the response of the system to the photoinduced charge separation. For example, photoexcitation of the Ru^{II}(α-diimine) chromophore in a $TiO_2-Rh^{III}-Ru^{II}$ heterotriad results in stepwise charge separation, the first electron-transfer step $TiO_2-Rh^{III}-{}^*Ru^{II} \rightarrow TiO_2-Rh^{II}-Ru^{III}$ having an efficiency close to unity.[14] Further charge separation via electron injection into the semiconductor is, however, only 40% efficient because of a competing charge-recombination process.

An important development in the multidisciplinary field of molecular photonic/electronic materials is the construction of high-performance "molecular-scale" computers,[15] incorporating devices capable of high-density data transport close to the speed of light. As photoinduced energy- and electron-transfer processes can occur on the subpicosecond time scale, the design of molecules performing switching (yes/no) and other logical operations via optical inputs has received considerable attention. Apart from the energy- or electron transfer processes themselves, switching of physical properties may also result from coupled selective bond-breaking or -making reactions. Reversible rearrangement processes in transition metal clusters selectively triggered by external stimuli such as light absorption or redox reaction,[16−20] together with extensive possibilities to functionalize the cluster core, make the molecular cluster systems (similar to functionalized metal nanoparticles[21,22] or carborane skeletons[23]) promising candidates for connector elements in nanoscale switchable junction devices. When a cluster is used as the active switchable component, the significant structural and electronic reorganization of the metal core triggered by an external stimulus may reversibly interrupt the electronic coupling between covalently bound donor and acceptor termini (Scheme 1). Alternatively, changing the electronic properties of the cluster junction by attachment of a redox active probe group may influence the electronic coupling between the donor and acceptor moieties in a similar way (Scheme 2). It has been our aim to realize the latter assembly. First of all, we have focused on the photochemical response of a cluster core to the varied redox state of an acceptor unit, examined without the donor and acceptor moieties attached.

Herein we report the redox-controlled photochemical reactivity of the novel cluster $[Os_3(CO)_{10}(AcPy\text{-}MV)]^{2+}$ (the dication AcPy-MV = AcPy-MV^{2+} = [2-pyridylacetimine-*N*-(2-(1′-methyl-4,4′-bipyridine-1,1′-diium-1-yl)ethyl)]-$(PF_6)_2$) (**1**$^{2+}$) (Chart 1). The strongly electron accepting 4,4′-

Scheme 1. Reversible Interruption of the Electronic Communication between Donor (D) and Acceptor (A) Termini in a Supramolecular System, Employing a Metal Cluster as the Active Switchable Component

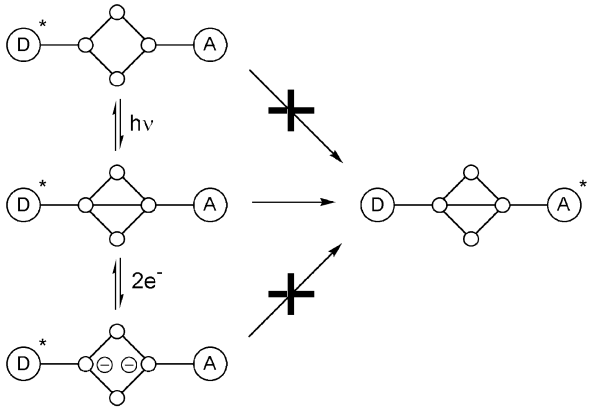

Scheme 2. Reversible Interruption of the Electronic Communication between Donor (D) and Acceptor (A) Termini by Attachment of a Reducible Electron Trap (T) to the Cluster Junction

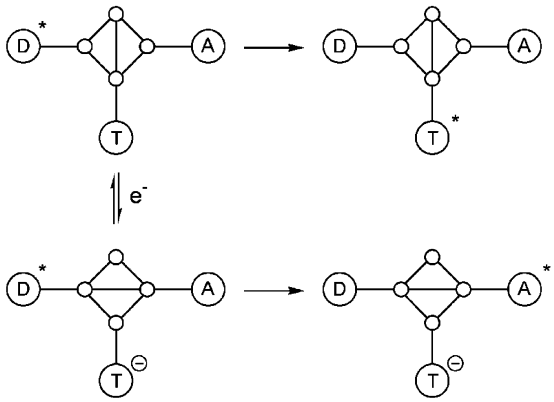

(4) Bignozzi, C. A.; Schoonhover, J. R.; Scandola, F. *Prog. Inorg. Chem.* **1997**, *44*, 1−95.
(5) Balzani, V.; Campagna, S.; Denti, G.; Juris, A.; Serroni, S.; Venturi, M. *Acc. Chem. Res.* **1998**, *31*, 26−34.
(6) Amadelli, R.; Argazzi, R.; Bignozzi, C. A.; Scandola, F. *J. Am. Chem. Soc.* **1990**, *112*, 7099−7103.
(7) Gust, D.; Moore, T. A.; Moore, A. L. *Acc. Chem. Res.* **1993**, *26*, 198−205.
(8) Harriman, A.; Sauvage, J. P. *Chem. Soc. Rev.* **1996**, *25*, 41−48.
(9) Liddell, P. A.; Kuciauskas, D.; Sumida, J. P.; Nash, B.; Nguyen, D.; Moore, A. L.; Moore, T. A.; Gust, D. *J. Am. Chem. Soc.* **1997**, *119*, 1400−1405.
(10) Slate, C. A.; Striplin, D. R.; Moss, J. A.; Chen, P.; Erickson, B. W.; Meyer, T. J. *J. Am. Chem. Soc.* **1998**, *120*, 4885−4886.
(11) Wasielewski, M. R. *Chem. Rev.* **1992**, *92*, 435−461.
(12) Gilat, S. L.; Kawai, S. H.; Lehn, J.-M. *J. Chem. Soc., Chem. Commun.* **1993**, 1439−1442.
(13) Heath, J. R.; Ratner, M. A. *Phys. Today* **2003**, *56*, 43−49.
(14) Kleverlaan, C. J.; Indelli, M. T.; Bignozzi, C. A.; Pavanin, L.; Scandola, F.; Hasselman, G. M.; Meyer, G. J. *J. Am. Chem. Soc.* **2000**, *122*, 2840−2849.
(15) Wada, Y. *Ann. N. Y. Acad. Sci.* **1998**, *852*, 257−276.
(16) Lemoine, P. *Coord. Chem. Rev.* **1982**, *47*, 55−88.
(17) Lemoine, P. *Coord. Chem. Rev.* **1988**, *83*, 169−197.
(18) Zanello, P. In *Structure and Bonding*; Clarke, M. J., Goodenough, J. B., Ibers, J. A., Jorgensen, C. K., Mingos, D. M. P., Neilands, J. B., Palmer, G. A., Reinen, D., Sadler, P. J., Weiss, R., Williams, R. J. P., Eds.; Springer: Berlin, 1992; Vol. 79, pp 101−214.
(19) Zanello, P.; de Biani, F. F. In *Metal Clusters in Chemistry*; Braunstein, P., Oro, L. A., Raithby, P. R., Eds.; Wiley-VCH: Weinheim, Germany, 1999; Vol. 2, pp 1104−1136.
(20) Vergeer, F. W.; Bakker, M. J.; Kleverlaan, C. J.; Hartl, F.; Stufkens, D. J. *Coord. Chem. Rev.* **2002**, *229*, 107−112.
(21) Gittins, D. I.; Bethell, D.; Schiffrin, D. J.; Nichols, R. J. *Nature* **2000**, *408*, 67−69.
(22) Pouthier, V.; Girardet, C. *Surf. Sci.* **2002**, *511*, 203−214.
(23) Fox, M. A.; Paterson, A. J.; Nervi, C.; Galeotti, F.; Puschmann, H.; Howard, J. A. K.; Low, P. J. *Chem. Commun.* **2001**, 1610−1611.

Chart 1. Schematic Structures of the Clusters [Os$_3$(CO)$_{10}$(α-diimine)] and the α-Diimine Ligands Used in This Study

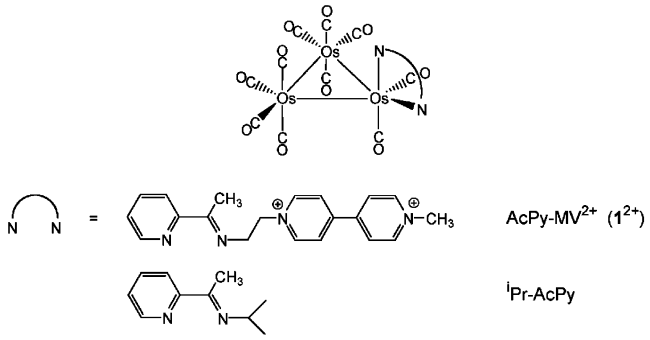

bipyridine-1,1′-diium (viologen) unit is covalently linked to the imine nitrogen of the α-diimine ligand.

Picosecond transient absorption and time-resolved infrared spectra were recorded to find out if photoinduced electron transfer to the remote viologen moiety and concomitant formation of a charge-separated state can compete with the fast decay of the initially populated $\sigma\pi^*$ excited state to the ground state and/or with the formation of biradical photoproducts.[20,24] Similar electron-transfer reactions were observed for several viologen-linked [Ru(bpy)$_3$]$^{2+}$ complexes[25−28] in the nanosecond time domain. In the second part, we will focus on the redox control of the charge separation in [Os$_3$(CO)$_{10}$(AcPy-MV)]$^{2+}$, with the aim to restore the photoreactivity of the ordinary [Os$_3$(CO)$_{10}$(α-diimine)] clusters.[20,29−31] As a proper reference, we have chosen the structurally closely related cluster [Os$_3$(CO)$_{10}$(^{i}Pr-AcPy)], where the alkyl-linked viologen unit is replaced by the isopropyl group (Chart 1).

Experimental Section

Materials and Preparation. [Os$_3$(CO)$_{12}$] (Strem Chemicals), 4,4′-bipyridine (Fluka), 1-(2-pyridinyl)ethanone (Acros), 2-bromoethylamine hydrobromide, piperidine (Aldrich), and ferrocene (BDH) were used as received. Trimethylamine *N*-oxide dihydrate, Me$_3$NO·2H$_2$O (Janssen), was dehydrated prior to use by vacuum sublimation. Solvents of analytical grade (Acros, EtOH, MeOH, hexane, diethyl ether, CH$_2$Cl$_2$, and acetonitrile; Aldrich, 2-chlorobutane (2-ClBu)) and spectroscopic grade (Acros, acetone) were dried over sodium (EtOH, MeOH, Et$_2$O, hexane), CaH$_2$ (CH$_2$Cl$_2$, MeCN, 2-ClBu), and B$_2$O$_3$ (acetone) and freshly distilled under a nitrogen atmosphere prior to use. Neutral aluminum oxide 90 (70−230 mesh; Merck) for column chromatography was activated by heating in vacuo at 450 K overnight and stored under N$_2$. The supporting electrolyte Bu$_4$NPF$_6$ (Aldrich) was recrystallized twice from ethanol and dried in vacuo at 350 K overnight.

Scheme 3. Synthesis of Cluster $\mathbf{1}^{2+}$

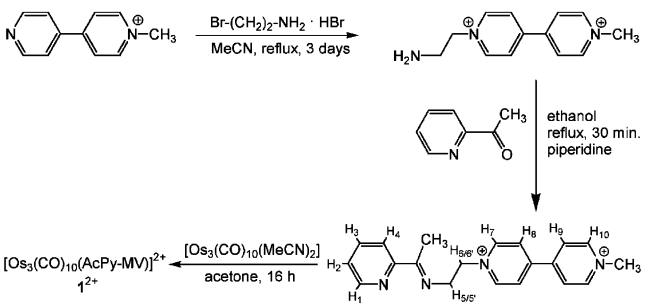

Synthetic Procedures. All syntheses were performed under an inert atmosphere of dry nitrogen, using standard Schlenk techniques. The starting compounds [1-methyl-4,4′-bipyridin-1-ium]I and [1-(2-aminoethyl)-1′-methyl-4,4′-bipyridine-1,1′-diium](PF$_6$)$_2$,[25] the precursor [Os$_3$(CO)$_{10}$(MeCN)$_2$],[32] and the reference cluster [Os$_3$(CO)$_{10}$(^{i}Pr-AcPy)][29] were prepared according to published procedures and identified by ^{1}H NMR and FTIR spectroscopies. The synthetic route toward cluster $\mathbf{1}^{2+}$ is depicted in Scheme 3.

Synthesis of [2-Pyridylacetimine-*N*-(2-(1′-methyl-4,4′-bipyridine-1,1′-diium-1-yl)ethyl)](PF$_6$)$_2$ (AcPy-MV^{2+}). A mixture of [1-(2-aminoethyl)-1′-methyl-4,4′-bipyridine-1,1′-diium](PF$_6$)$_2$ (385 mg, 0.76 mmol), 1-(2-pyridinyl)ethanone (0.2 mL, 1.8 mmol), and piperidine (a few drops) in EtOH (10 mL) was refluxed for 1.5 h in the presence of 3 Å molecular sieves. After this period the solvent was removed in vacuo and the residue was washed with Et$_2$O (5 × 10 mL). The ligand was isolated as an off-white solid in 66% yield. ^{1}H NMR (acetone-d_6, 293 K) (for numbering see Scheme 3): δ 9.59 (d, ^3J = 6.6 Hz, 2H, H$_7$), 9.36 (d, ^3J = 6.6 Hz, 2H, H$_{10}$), 8.87 (d, ^3J = 6.6 Hz, 2H, H$_8$), 8.81 (d, ^3J = 6.6 Hz, 2H, H$_9$), 8.66 (d, ^3J = 4.5 Hz, 1H, H$_1$), 8.21 (d, ^3J = 8 Hz, 1H, H$_4$), 7.94 (dd, ^3J = 8 Hz, ^3J = 7.5 Hz, 1H, H$_3$), 7.56 (dd, ^3J = 4.5 Hz, ^3J = 7.5 Hz, 1H, H$_2$), 5.41 (t, ^3J = 5.1 Hz, 2H, H$_6$), 4.74 (s, 3H, N−CH$_3$), 4.36 (t, ^3J = 5.1 Hz, 2H, H$_5$), 2.49 (s, 3H, C−CH$_3$). FAB$^+$ MS (*m*/*z*): 631.1, [M + Na]$^+$; 463.1, [M − PF$_6$]$^+$ (calcd *m*/*z* 463.1); 318.2, [M − 2PF$_6$]$^+$.

Synthesis of [Os$_3$(CO)$_{10}$(AcPy-MV)]$^{2+}$(PF$_6$)$_2$ ($\mathbf{1}^{2+}$). A solution of [Os$_3$(CO)$_{10}$(MeCN)$_2$] (220 mg, 0.24 mmol) and AcPy-MV^{2+} (230 mg, 0.37 mmol) in acetone (25 mL) was stirred in the dark for 16 h. After this period the solvent was removed in vacuo. The crude product was purified by column chromatography over aluminum oxide, using CH$_2$Cl$_2$/MeCN gradient elution. Cluster $\mathbf{1}^{2+}$ was obtained as a deep red solid in 20% yield. IR [ν(CO); MeCN]: 2089 (m), 2040 (s), 2002 (vs), 1986 (s, sh), 1964 (m, sh), 1948 (m, sh), 1893 (w) cm^{-1}. ^{1}H NMR (acetone-d_6, 293 K) (for numbering see Scheme 3): δ 9.57 (d, ^3J = 5.4 Hz, 1H, H$_1$), 9.50 (d, ^3J = 7.2 Hz, 2H, H$_7$), 9.39 (d, ^3J = 6.9 Hz, 2H, H$_{10}$), 8.89 (d, ^3J = 7.2 Hz, 2H, H$_8$), 8.78 (d, ^3J = 6.9 Hz, 2H, H$_9$), 8.54 (d, ^3J = 7.9 Hz, 1H, H$_4$), 8.19 (dd, ^3J = 7.5 Hz, ^3J = 8.1 Hz, 1H, H$_3$), 7.58 (dd, ^3J = 7.5 Hz, ^3J = 5.7 Hz, 1H, H$_2$), 5.65 (ddd, ^2J = 13 Hz, ^3J = 4.2 Hz, ^3J = 3.9 Hz, 1H, H$_{6/6'}$), 5.50 (ddd, ^2J = 14 Hz, ^3J = 4.2 Hz, ^3J = 3.9 Hz, 1H, H$_{5/5'}$), 5.41 (ddd, ^2J = 13 Hz, ^3J = 9.6 Hz, ^3J = 3.9 Hz, 1H, H$_{6/6'}$), 5.02 (ddd, ^2J = 14 Hz, ^3J = 9.6 Hz, ^3J = 3.9 Hz, 1H, H$_{5/5'}$), 4.75 (s, 3H, N−CH$_3$), 3.08 (s, 3H, C−CH$_3$). UV−vis (acetone): 373 (sh), 554 nm. FAB$^+$ MS (*m*/*z*): 1482, (M

(24) Vergeer, F. W.; Kleverlaan, C. J.; Stufkens, D. J. *Inorg. Chim. Acta* **2002**, *327*, 126−133.
(25) Kelly, L. A.; Rodgers, M. A. J. *J. Phys. Chem.* **1994**, *98*, 6386−6391.
(26) Kelly, L. A.; Rodgers, M. A. J. *J. Phys. Chem.* **1995**, *99*, 13132−13140.
(27) Yonemoto, E. H.; Riley, R. L.; Kim, Y. I.; Atherton, S. J.; Schmehl, R. H.; Mallouk, T. E. *J. Am. Chem. Soc.* **1992**, *114*, 8081−8087.
(28) Yonemoto, E. H.; Saupe, G. B.; Schmehl, R. H.; Hubig, S. M.; Riley, R. L.; Iverson, B. L.; Mallouk, T. E. *J. Am. Chem. Soc.* **1994**, *116*, 4786−4795.
(29) Nijhoff, J.; Bakker, M. J.; Hartl, F.; Stufkens, D. J.; Fu, W.-F.; van Eldik, R. *Inorg. Chem.* **1998**, *37*, 661−668.
(30) Nijhoff, J.; Hartl, F.; Stufkens, D. J.; Fraanje, J. *Organometallics* **1999**, *18*, 4380−4389.
(31) Nijhoff, J.; Hartl, F.; van Outersterp, J. W. M.; Stufkens, D. J.; Calhorda, M. J.; Veiros, L. F. *J. Organomet. Chem.* **1999**, *573*, 121−133.
(32) Zoet, R.; Jastrzebski, J. T. B. H.; van Koten, G.; Mahabiersing, T.; Vrieze, K.; Heijdenrijk, D.; Stam, C. H. *Organometallics* **1988**, *7*, 2108−2117.

$+ Na)^+$; 1315.5, $(M - PF_6)^+$ (calcd *m*/*z* 1315.0); 1170, $(M - 2PF_6)^+$.

Spectroscopic Measurements. FTIR spectra were recorded on Bio-Rad FTS-7 and Bio-Rad FTS-60A spectrometers (16 scans at 2 cm^{-1} resolution), the latter being equipped with a dual-source rapid-scan 896 interferometer and a nitrogen-cooled MCT detector. The sample compartment of the Bio-Rad FTS-60A spectrometer was modified to allow laser irradiation into a thermostated cell. Electronic absorption spectra were recorded on a Hewlett-Packard 8453 diode-array spectrophotometer, ^1H NMR spectra on a Bruker AMX 300 spectrometer, and fast atom bombardment (FAB) mass spectra on a JEOL JMS SX/SX102A spectrometer.

Photochemistry. The 514.5 nm line of a Spectra Physics model 2016 argon-ion laser was used for the continuous-wave irradiation experiments. Low-temperature IR measurements were performed with an Oxford Instruments DN 1704/54 liquid-nitrogen-cooled cryostat equipped with CaF_2 windows. All photochemical samples were prepared under a nitrogen atmosphere, using standard inert-gas techniques. The cluster concentration was $10^{-3}-10^{-4}$ mol dm^{-3}.

Nanosecond transient absorption (ns TA) spectra were obtained by irradiating the samples with 2 ns pulses of the 550 nm line (typically 4 mJ $pulse^{-1}$) of a tunable (420−710 nm) Coherent Infinity XPO laser. The probe light from a low-pressure, high-power EG&G FX-504 Xe lamp was passed through the sample cell and dispersed by an Acton Spectra-Pro-150 spectrograph equipped with 150 g mm^{-1} or 600 g mm^{-1} grating and a tunable slit (1−500 μm), resulting in a 6 or 1.2 nm maximum resolution, respectively. The data collection system consisted of a gated intensified CCD detector (Princeton Instruments ICCD-576EMG/RB), a programmable pulse generator (PG-200), and an EG&G Princeton Applied Research model 9650 digital delay generator.

Picosecond transient absorption (ps TA) spectra were recorded using the setup installed at the University of Amsterdam.[24] Part of the 800 nm output of a Ti−sapphire regenerative amplifier (1 kHz, 130 fs, 1 mJ) was focused into a H_2O flow-through cell (10 mm; Hellma) to generate white light. The residual part of the 800 nm fundamental was used to provide 505 nm (fourth harmonic of the 2020 OPA idler beam) excitation pulses with a general output of 3−5 μJ $pulse^{-1}$. After passing through the sample, the probe beam was coupled into a 400 μm optical fiber and detected by a CCD spectrometer (Ocean Optics, PC2000). The chopper (Rofin Ltd., f = 10−20 Hz) was placed in the excitation beam and provided I and I_0, in dependence on its status (open or closed). The excited-state spectra were obtained by $\Delta A = \log(I/I_0)$. Typically two thousand excitation pulses were averaged to obtain the transient at a particular time delay. For the single-wavelength kinetic measurements, a second OPA was used to generate probe pulses at the desired wavelength, while an amplified Si photodiode (New-Port, 818 UV/4832-C) was used for detection. The output of the Si photodiode was conducted to an AD-converter (National Instruments, PCI 4451, 205 kS s^{-1}), which enabled the measurement of the intensity of each separate pulse. Typically 500 excitation pulses were averaged to obtain the transient at a particular time delay. The sample solutions for the ps TA measurements were placed under nitrogen in 2 mm quartz cuvettes (Hellma) and had an optical density between 0.8 and 1.0 at the excitation wavelength.

Picosecond time-resolved infrared (ps TRIR) spectra were recorded using the Picosecond Infrared Absorption and Transient Excitation (PIRATE) facility at the Rutherford Appleton Laboratory.[33] The laser system is based on a Ti−sapphire regenerative amplifier (Spectra Physics/Positive Light, Superspitfire), operating at 1 kHz repetition rate at ca. 800 nm, with energy of 2−3 mJ $pulse^{-1}$ (150 fs fwhm). Tunable mid-IR outputs (150−200 cm^{-1} fwhm, 200 fs) were generated by frequency-down conversion of the signal and idler outputs of a white-light seeded, 800 nm pumped BBO OPA in an $AgGaS_2$ crystal. Second harmonic generation of the residual fundamental light (800 nm) provided 400 nm pulses, which were used to pump a second OPA, generating 500 nm excitation pulses. The mid-IR beam generated by the first OPA was split into reference and probe beams, using a 50% germanium beam-splitter. The flow-through cell, consisting of two CaF_2 windows separated by 0.25−1 mm spacers, was allowed to make a rastering movement perpendicular to the probe beam to avoid local heating and sample decomposition by the laser beams. Two separate 64-element HgCdTe linear array detectors (MCT-13-64el (Infrared Associates Inc.) and MCT-64000 preamplifiers (Infrared Systems Development Corp.)) were used to detect the mid-IR reference and probe signals. TRIR spectra comprising the whole CO-stretching region (2200−1700 cm^{-1}) were constructed by precise overlap of three or four 150 cm^{-1} windows. Calibration of the spectra was established by comparing the parent bleach positions with the peak positions of the corresponding ν(CO) bands in the regular FTIR spectra. The samples for the ps TRIR measurements had an optical density between 0.8 and 0.9 at the excitation wavelength.

Electrochemistry. Cyclic voltammograms (CV) of 10^{-3} M cluster $\mathbf{1}^{2+}$ in 10^{-1} M Bu_4NPF_6 electrolyte solution were recorded in a gastight, single-compartment, three-electrode cell equipped with platinum disk working (apparent surface area of 0.42 mm^2), coiled platinum wire auxiliary, and silver wire pseudoreference electrodes. The cell was connected to a computer-controlled PAR model 283 potentiostat. All redox potentials are reported against the ferrocene/ferrocenium (Fc/Fc^+) redox couple used as an internal standard.[34,35] IR and UV−vis spectroelectrochemical experiments were performed with optically transparent thin-layer electrochemical (OTTLE) cells[36,37] equipped with a Pt minigrid working electrode (32 wires per cm) and CaF_2 windows. The potential during the thin-layer electrolyses was controlled by a PA4 (EKOM, Polná, Czech Republic) potentiostat. The cluster concentration in the spectroelectrochemical samples varied from 1×10^{-3} mol dm^{-3} (UV−vis) to 5×10^{-3} mol dm^{-3} (IR).

Results and Discussion

Synthesis of $[Os_3(CO)_{10}(AcPy\text{-}MV)]^{2+}$ ($\mathbf{1}^{2+}$). The novel cluster $[Os_3(CO)_{10}(AcPy\text{-}MV)]^{2+}$ ($\mathbf{1}^{2+}$) was synthesized via a three-step reaction sequence (see Scheme 3). The IR spectrum of $\mathbf{1}^{2+}$ in MeCN closely resembles that of the reference compound $[Os_3(CO)_{10}(^iPr\text{-}AcPy)]$ (**2**),[29] the ν(CO) bands being slightly shifted to larger wavenumbers. This difference is attributed to a slightly decreased π-back-bonding toward the carbonyl ligands due to the reduced basicity of the $AcPy\text{-}MV^{2+}$ ligand. The ^1H NMR spectrum of $\mathbf{1}^{2+}$ in acetone-d_6 shows the characteristic resonances of the methyl viologen unit and the ethylene linkage. In accordance with

(33) Towrie, M.; Grills, D. C.; Dyer, J.; Weinstein, J. A.; Matousek, P.; Barton, R.; Bailey, P. D.; Subramaniam, N.; Kwok, W. M.; Ma, C.; Phillips, D.; Parker, A. W.; George, M. W. *Appl. Spectrosc.* **2003**, *57*, 367−380.
(34) Pavlishchuk, V. V.; Addison, A. W. *Inorg. Chim. Acta* **2000**, *298*, 97−102.
(35) Gritzner, G.; Kůta, J. *Pure Appl. Chem.* **1984**, *56*, 461−466.
(36) Krejčík, M.; Daněk, M.; Hartl, F. *J. Electroanal. Chem., Interfacial Electrochem.* **1991**, *317*, 179−187.
(37) Hartl, F.; Luyten, H.; Nieuwenhuis, H. A.; Schoemaker, G. C. *Appl. Spectrosc.* **1994**, *48*, 1522−1528.

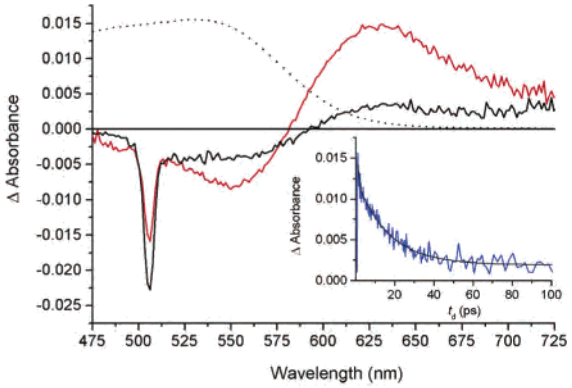

Figure 1. Transient difference-absorption spectra of the reference cluster [Os$_3$(CO)$_{10}$(^{i}Pr-AcPy)] in acetone measured at time delays of 1 ps (red color) and 70 ps (black color), respectively, after 130 fs fwhm excitation at 505 nm, together with the ground-state electronic spectrum in acetone (dotted line). Inset: Experimental (blue color) and fitted (black color) kinetic profile of the difference absorbance of [Os$_3$(CO)$_{10}$(^{i}Pr-AcPy)] in acetone at 630 nm, after 130 fs fwhm excitation at 505 nm.

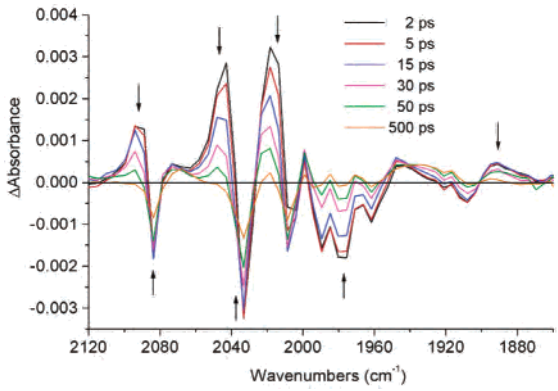

Figure 2. Difference-absorption ps TRIR spectra of [Os$_3$(CO)$_{10}$(^{i}Pr-AcPy)] in 2-ClBu at 2, 5, 15, 30, 50, and 500 ps after 500 nm excitation (ca. 150 fs fwhm, 5 μJ pulse^{-1}).

the electron-accepting character of the viologen moiety, the signals of the AcPy protons are slightly shifted to lower field compared to those of [Os$_3$(CO)$_{10}$(^{i}Pr-AcPy)]. The chelating coordination of the AcPy-MV^{2+} ligand to the cluster core (Chart 1) was further confirmed by the FAB$^+$ mass spectrum of **1**$^{2+}$.

Electronic Absorption Spectra of [Os$_3$(CO)$_{10}$(AcPy-MV)]$^{2+}$ (1^{2+}). The UV−vis absorption spectrum of cluster **1**$^{2+}$ exhibits a dominant lowest-energy band, with its maximum shifted from 554 nm in acetone to 576 nm in CH_2Cl_2. Similar to [Os$_3$(CO)$_{10}$(^{i}Pr-AcPy)],[38,39] it belongs to several charge-transfer transitions from different orbitals of the triosmium core to the α-diimine ligand, denoted as σ(Os−Os) → π*(α-diimine). Irradiation into this band will therefore result in the population of the lowest $\sigma\pi$* excited state and weaken at least one of the Os−Os(α-diimine) bonds.[39] The small red shift of the lowest-energy band of **1**$^{2+}$ compared to [Os$_3$(CO)$_{10}$(^{i}Pr-AcPy)] (λ_{max} = 536 nm in acetone) is attributed to a decreased energy of the lowest π*(AcPy) orbital due to the attached electron-withdrawing methyl viologen moiety.

Picosecond Transient Absorption Spectra of the Reference Cluster [Os$_3$(CO)$_{10}$(^{i}Pr-AcPy)]. The ps TA spectra of [Os$_3$(CO)$_{10}$(^{i}Pr-AcPy)] in 2-chlorobutane (2-ClBu), dichloromethane, THF, and MeCN have been reported in detail elsewhere.[20,24] Here we describe the measurements in acetone, as this solvent was also used for cluster **1**$^{2+}$ (vide infra).

Excitation of [Os$_3$(CO)$_{10}$(^{i}Pr-AcPy)] with the 505 nm laser pulse resulted in the appearance of a bleach at 550 nm (Figure 1), which is close to the maximum of the ground-state lowest-energy absorption band of the cluster in acetone (536 nm). At the time delay t_d = 1 ps, the observed intense transient absorption with an apparent maximum at 630 nm (Figure 1) belongs to the $\sigma\pi$* excited state, based on the comparison with the reported ps TA spectra in the other solvents. The $\sigma\pi$* transient decays with a lifetime τ_1 = 17 ± 2 ps, similar to the bleach decay probed at 550 nm. At t_d = 70 ps, the TA spectrum still shows the presence of the ground-state bleach that diminished to 45% of the initial signal (Figure 1). The $\sigma\pi$* transient partly converted during this time into a new species absorbing in the long-wavelength region (600−800 nm). This reminiscent unresolved broad absorption is characteristic[20,24] for the biradical photoproduct [$^{\bullet}$Os(CO)$_4$−Os(CO)$_4$−$^+$Os(Sv)(CO)$_2$(^{i}Pr-AcPy$^{\bullet-}$)] (Sv = coordinating solvent). The $\sigma\pi$* transient decay has also an ultrafast component τ_2 = 0.8 ± 0.5 ps (τ_1/τ_2 ratio 3:1), which probably corresponds to conversion of a part of the excited cluster molecules into the biradicals from a nonrelaxed $\sigma\pi$* excited state.[20,24] The limited quantum yield for the formation of the acetone-stabilized biradicals has its origin in branching between the decay to the ground state and crossing a barrier from the relaxed ("triplet") $\sigma\pi$* excited state to a dissociative state. The barrier in acetone is probably lower compared with 2-ClBu where the relaxed $\sigma\pi$* state of [Os$_3$(CO)$_{10}$(^{i}Pr-AcPy)] lives 25 ± 2 ps and the concomitant ground-state recovery is more extensive.[20,24]

Picosecond Time-Resolved IR Spectra of the Reference Cluster [Os$_3$(CO)$_{10}$(^{i}Pr-AcPy)]. After irradiation into the lowest-energy visible absorption band of [Os$_3$(CO)$_{10}$(^{i}Pr-AcPy)] in *noncoordinating* 2-ClBu, the TRIR spectra at early time delays (<3 ps) display instantaneous bleaching of the parent ν(CO) bands (Figure 2). At the same time, broad transient absorption bands are observed with maxima around 2089 and 2028 cm^{-1} (the maximum of the latter band is estimated from the line shapes at the low- and high-frequency sides of the 2033 cm^{-1} bleach), together with small transient bands at 1999, 1948, and 1891 cm^{-1}, all belonging to the excited state of [Os$_3$(CO)$_{10}$(^{i}Pr-AcPy)]. Thus, the highest-frequency ground-state band at 2083 cm^{-1}, which partially overlaps with the corresponding transient feature, is clearly shifted to higher frequency (2089 cm^{-1}) in the excited state. This is in line with its predominant $\sigma\pi$* character[24,38,39] and a slightly decreased π-back-donation to the carbonyl ligands. On a longer time scale (up to 100 ps) the initially observed ν(CO) bands decay and small remaining bands at 2068, 2018, 1999, 1985, and 1971 cm^{-1} and a broad absorption between 1950 and 1910 cm^{-1} indicate the formation of a

(38) Calhorda, M. J.; Hunstock, E.; Veiros, L. F.; Hartl, F. *Eur. J. Inorg. Chem.* **2001**, 223−231.
(39) Bakker, M. J.; Calhorda, M. J.; Hartl, F. Manuscript in preparation.

long-lived primary photoproduct. In accordance with TA experiments on $[Os_3(CO)_{10}(^iPr\text{-}AcPy)]$ on the picosecond time scale (vide supra), the latter photoproduct is assigned to the open-structure biradical $[^{\bullet}Os(CO)_4{-}Os(CO)_4{-}^{+}Os(CO)_2(^iPr\text{-}AcPy^{\bullet-})]$. This assignment is further confirmed by the close correspondence between the resulting ps TRIR spectrum at the time delay $t_d = 500$ ps and the reported ns TRIR spectrum of $[Os_3(CO)_{10}(^iPr\text{-}AcPy)]$ in 2-ClBu at $t_d =$ 40 ns.[40] Upon decay of the excited-state absorption bands also the parent bleaches fade away. The remaining TRIR spectrum at $t_d = 500$ ps shows the parent bleaches at 2083 and 2033 cm^{-1} at ca. 40% of their initial intensity, which is close to the 30% observed in the corresponding ps TA experiment in the same solvent.[24] As the overlap between the ground- and excited-state ν(CO) bands does not change on the picosecond time scale, the parent-bleach recovery in the TRIR experiments provides another proof that ca. 60% of the excited molecules directly decays to the ground state. Moreover, as the transient absorption bands do not shift, the excited-state lifetime can be estimated by plotting the IR intensities at 2043 and 2018 cm^{-1} against time, resulting in monoexponential decays with lifetimes of 21.1 and 25.5 ps, respectively. These excited-state lifetimes are also in good agreement with the value obtained[24] from single-wavelength TA experiments in 2-ClBu (25 ± 2 ps).

Excitation of $[Os_3(CO)_{10}(^iPr\text{-}AcPy)]$ in *strongly coordinating* acetonitrile results in ps TRIR spectra that are initially very similar to those obtained in 2-ClBu. Again, the first spectra after the excitation display instantaneous bleaching of the parent ν(CO) bands but the transient absorption bands are significantly broader than in 2-ClBu due to interactions of the solvent with the excited cluster. At longer time delays (up to 100 ps) the excited-state ν(CO) bands decay and, just as in 2-ClBu, small remaining bands at 2058 and 2008 cm^{-1} together with a broad absorption between 1955 and 1895 cm^{-1} (cf. Figure 3a,b) indicate the formation of open-structure biradicals (Scheme 4). The generally smaller ν(CO) wavenumbers for the biradicals in MeCN reveal coordination of the solvent molecules that increases electron density at the cluster core and the π-back-donation to the carbonyl ligands. However, unlike in 2-ClBu, the *biradicals* are not the only photoproducts in MeCN. This is concluded from the observation that the transient lowest-frequency IR band (Figure 2) does not decay to the baseline. Instead, its intensity increases on longer time scales, resulting in a distinct band at 1877 cm^{-1} at $t_d = 100$ ps. At the same time, an additional absorption band rises at 1965 cm^{-1} (Figure 3b). Importantly, similar transient ν(CO) bands were observed at 1971 and 1983 cm^{-1} in rapid-scan FTIR spectra of $[Os_3(CO)_{10}(^iPr\text{-}AcPy)]$ in MeCN on the time scale of seconds, which were attributed to open-structure *zwitterions* $[^{-}Os(CO)_4{-}Os(CO)_4{-}^{+}Os(Sv)(CO)_2(\alpha\text{-diimine})]$ (Sv = MeCN)[29] (see Figure 3c). The TRIR spectra of $[Os_3(CO)_{10}(^iPr\text{-}AcPy)]$ in MeCN thus unambiguously prove, for the first time, that zwitterions are already present in the ps time domain, being most likely formed directly from a $\sigma\pi^*$ excited state (Scheme 4). This conclusion agrees with the earlier reported[24] ps TA data.

Scheme 4. Schematic Representation of the Photoprocesses of the Reference Cluster $[Os_3(CO)_{10}(^iPr\text{-}AcPy)]$[a]

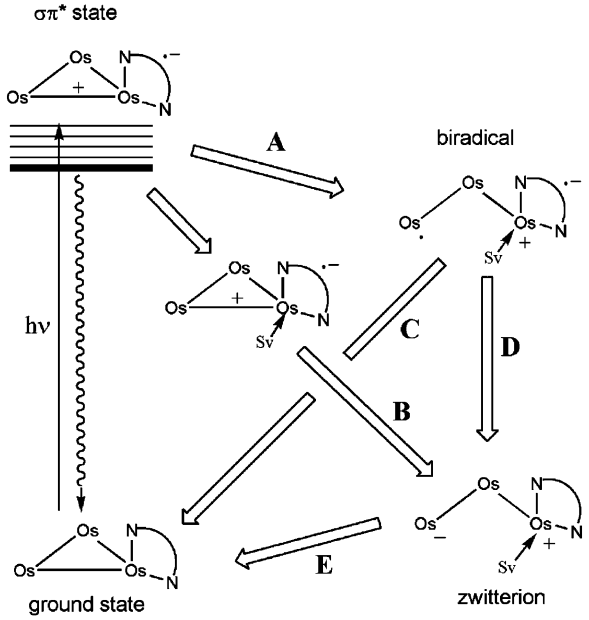

[a] The separate reactions steps A−E strongly depend on the solvent (Sv) used. Process A: $\tau = 25$ ps, $\Phi = 0.4$ (2-ClBu); $\tau = 17$ ps, $\Phi = 0.6$ (acetone). Process B: $\tau = 3$ ps (acetonitrile). Process C: $\tau = 22$ ns (2-ClBu); $\tau = 677$ ns (acetone). Process D: $\tau = 19.7$ μs (acetonitrile); $\tau =$ 13.5 μs (2-ClBu + 1.0 M acetonitrile); $\tau = 12.9$ μs (2-ClBu + 1.0 M 1-octene). Process E: $\tau = 38$ s (acetonitrile); $\tau = 339$ ms (2-ClBu + 1.0 M 1-octene).

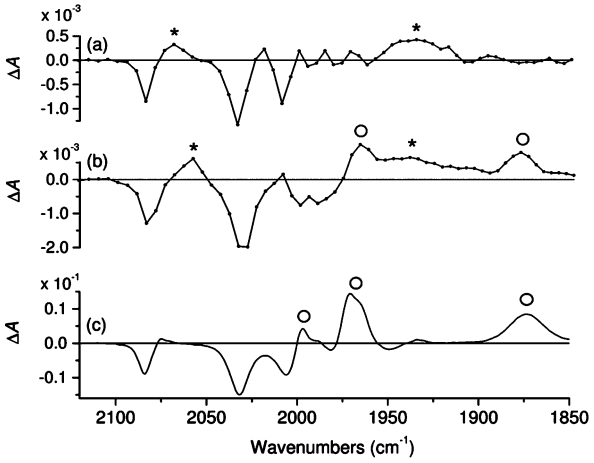

Figure 3. Difference-absorption IR spectra of $[Os_3(CO)_{10}(^iPr\text{-}AcPy)]$ (a) in 2-ClBu at $t_d = 500$ ps after 500 nm excitation, (b) in MeCN at $t_d = 100$ ps after 500 nm excitation, and (c) in MeCN at $t_d = 2.5$ s after 532 nm excitation. The asterisks denote ν(CO) bands of the solvent-stabilized biradicals, and the open circles MeCN-stabilized zwitterions.

The ps TRIR spectra of $[Os_3(CO)_{10}(^iPr\text{-}AcPy)]$ in *weakly coordinating* acetone closely resemble those obtained in noncoordinating 2-ClBu, the open-structure biradicals being at room temperature the only observable photoproducts (Scheme 4). In line with the moderate coordinating ability of the solvent, the ν(CO) wavenumbers of the acetone-stabilized biradicals lie between those determined in non-coordinating 2-ClBu and strongly coordinating MeCN,

(40) Bakker, M. J.; Hartl, F.; Stufkens, D. J.; Jina, O. S.; Sun, X.-Z.; George, M. W. *Organometallics* **2000**, *19*, 4310−4319.

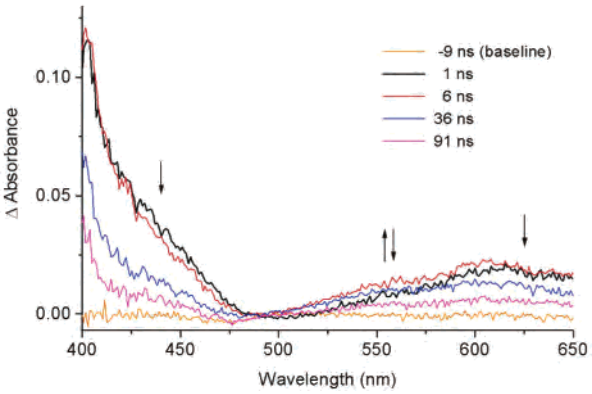

Figure 4. Transient difference-absorption spectra of cluster $\mathbf{1}^{2+}$ in acetone measured at time delays of −9 (baseline), 1, 6, 36, and 91 ps, respectively, after 130 fs fwhm excitation at 505 nm.

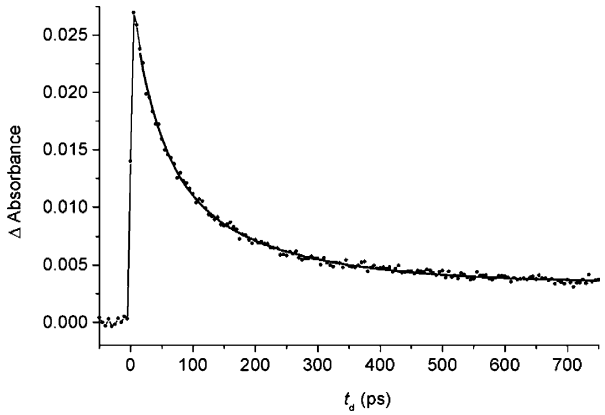

Figure 5. Kinetic profile of the difference absorbance of cluster $\mathbf{1}^{2+}$ in acetone at 600 nm, after 130 fs fwhm excitation at 505 nm.

reflecting a slight increase in the π-back-donation to the carbonyl ligands compared to 2-ClBu. The spectra at early time delays again display broad transient absorptions due to the $\sigma\pi^*$ excited state (see Figure 6a) and are used as a reference in the TRIR experiments with cluster $\mathbf{1}^{2+}$ in acetone described below. Differently from the situation in 2-ClBu (vide supra) and in agreement with the results of the ps TA measurements, the bleaches of the parent cluster [$Os_3(CO)_{10}$(^{i}Pr-AcPy)] in acetone decayed at $t_d = 500$ ps merely to 60% of their initial intensity. The quantum yield of the solvent-stabilized biradicals can therefore be estimated to amount to 0.6 in acetone but merely 0.4 in 2-ClBu. These values determined from the ps TRIR spectra are more accurate than those from the ps TA experiments (>0.45 and >0.30, respectively) due to the partial overlap of the parent bleach at 550 nm with the absorptions of the $\sigma\pi^*$ excited state and the biradical photoproduct in the latter case.

Picosecond Transient Absorption Spectra of the Dyad [$Os_3(CO)_{10}$(AcPy-MV)]$^{2+}$ ($\mathbf{1}^{2+}$). Picosecond transient absorption (ps TA) spectra of cluster $\mathbf{1}^{2+}$ in acetone were obtained by excitation at 505 nm and detection of the spectral changes in the wavelength region 400−650 nm. Kinetic profiles were probed at 560 nm in 200 fs intervals up to 10 ps and at 600 nm in 5 ps intervals up to 750 ps. The TA spectra measured at 1−91 ps after the 130 fs laser pulse are depicted in Figure 4. The kinetic profile of $\mathbf{1}^{2+}$, probed at 600 nm, is shown in Figure 5.

The TA spectrum at the pump−probe time delay $t_d = 1$ ps (Figure 4) shows an intense absorption at ca. 400 nm and a broad long-wavelength absorption with a maximum at about 615 nm. The observed absorption bands are characteristic for the one-electron-reduced methyl viologen ($MV^{\bullet+}$) unit[41] and are therefore attributed, in accordance with the results of the picosecond TRIR experiments (vide infra), to a charge-separated (CS) state in which an electron has been transferred from the cluster core to the lowest π^* orbital of the viologen moiety. Within the first 6 ps, the TA spectra show increasing absorbance in the region 500−610 nm. These spectral changes correspond to the continued population of the viologen-localized CS state, most likely via oxidative quenching of the initially populated $\sigma\pi^*$ excited state.[24,38] A similar situation exists for MLCT/CS states in several [Ru(R-bpy)$_2$(bpy-MV)]$^{4+}$ complexes, where a methyl viologen unit (MV^{2+}) is covalently linked at the 4-position of one of the 2,2′-bipyridine (bpy) ligands.[25−28,42] The bleached lowest-energy absorption band of cluster $\mathbf{1}^{2+}$ between 450 and 650 nm is obscured by the stronger absorption of the $MV^{\bullet+}$ transient in this region (Figure 9 (left part); vide infra). On a longer time scale (up to 300 ps), the transient absorption due to the temporarily reduced $MV^{\bullet+}$ unit decays biexponentially with ∼87% regeneration of parent cluster $\mathbf{1}^{2+}$. The latter process corresponds to the back electron transfer from the reduced viologen moiety to the oxidized cluster core.

The kinetics of the viologen-localized CS state was studied in more detail by evaluation of absorbance−time profiles. Provided population of the CS state indeed takes place via fast decay of the optically populated $\sigma\pi^*$ excited state (vide infra), the forward electron-transfer rate constant (k_f) can be derived from a single-exponential fit to the latter process. Unfortunately, an extensive overlap between the transient absorption band in the visible, belonging to the $\sigma\pi^*$ excited state (cf. the reference spectrum in Figure 1), and the characteristic composed absorption of the methyl viologen radical cation[41] (Figure 4 ($t_d = 6$ ps); cf. Figure 9 (left part)) prevents the lifetime of the $\sigma\pi^*$ excited state to be determined accurately by the TA spectroscopy. However, as the absorbance−time profile of $\mathbf{1}^{2+}$, probed at 560 nm, shows no further increase of the absorption due to the viologen radical cation ($MV^{\bullet+}$) after 10 ps, the viologen-localized CS state is most likely formed completely within this period. On the basis of this assumption, the rate constant k_f is estimated to have a lower limit of 4×10^{11} s^{-1}. As the photoinduced forward electron-transfer reaction is much faster than the decay of the CS state, the back-electron-transfer rate constant (k_b) may be obtained from the decay kinetics of the 606 nm band (Figure 5). The latter band decays biexponentially with lifetimes of 38 ± 3 ps (55%) and 166 ± 9 ps (45%) that correspond to back-electron-transfer rate constants $k_b = 2.6 \times 10^{10}$ and 6.0×10^9 s^{-1},

(41) Kosower, E. M.; Cotter, J. L. *J. Am. Chem. Soc.* **1964**, *86*, 5524−5527.

(42) Lomoth, R.; Häupl, T.; Johansson, O.; Hammarström, L. *Chem. Eur. J.* **2002**, *8*, 102−110.

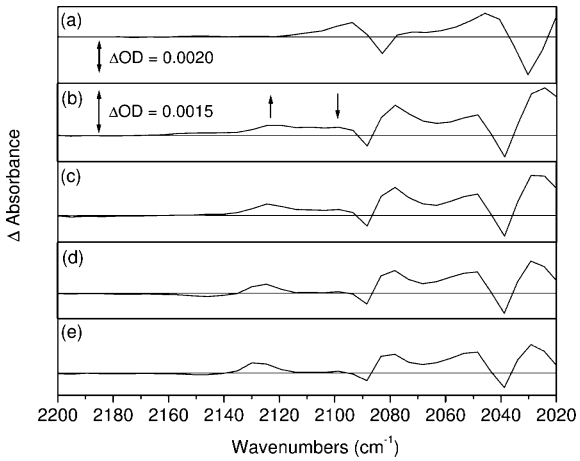

Figure 6. (a) Difference-absorption ps TRIR spectrum of the reference $[Os_3(CO)_{10}(^i$Pr-AcPy)] in acetone at $t_d = 3$ ps after 500 nm excitation (ca. 150 fs fwhm, 5 μJ pulse^{-1}) and (b−e) difference ps TRIR spectra of cluster $\mathbf{1}^{2+}$ in acetone at (b) 1, (c) 2, (d) 5, and (e) 15 ps after 500 nm excitation (ca. 150 fs fwhm, 5 μJ pulse^{-1}).

respectively. The biexponential kinetics could reflect a dynamical coupling between the $\sigma\pi^*$ and CS states (Scheme 4; vide infra) that are not in thermal equilibrium, the distribution between them being time-dependent. Population of the $\sigma\pi^*$ state also results in some Os−Os(AcPy) bond homolysis and formation of corresponding solvent-stabilized open-core biradicals, similar to the behavior of the reference cluster $[Os_3(CO)_{10}(^i$Pr-AcPy)] (vide supra). As their lifetime extends to the ns−μs time scale (cf. 677 ns for $[Os_3(CO)_{10}(^i$Pr-AcPy)] in acetone), the formation of the biradicals accounts for the 13% residual absorbance in Figure 5 observed after the decay of the CS state to the ground state ($t_d = 700$ ps).

Picosecond Time-Resolved IR Spectra of the Dyad $[Os_3(CO)_{10}$(AcPy-MV)]$^{2+}$ ($\mathbf{1}^{2+}$). The transient UV−vis spectra provide only limited information about the forward electron-transfer kinetics and the pathways to the CS state (major) and the open-core biradicals (minor). For this reason, the primary events after the photoexcitation of cluster $\mathbf{1}^{2+}$ in acetone with 500 nm light were studied with picosecond time-resolved infrared (ps TRIR) spectroscopy. The ps TRIR spectra were recorded at several pump−probe delays between 0 and 500 ps. Representative difference-absorption TRIR spectra are shown in Figure 6 and compared with those of the reference cluster $[Os_3(CO)_{10}(^i$Pr-AcPy)] in 2-ClBu (Figure 2) and acetone (Figure 6a). Due to the low symmetry of both decacarbonyl clusters, their ground-state IR spectra display a complicated ν(CO) band pattern. Extensive overlap between the bleached ν(CO) bands of the parent complexes and the transient absorption bands of their excited states precludes the determination of the excited-state CO-stretching frequencies to a large extent. Therefore, only the well-separated highest-frequency ν(CO) bands at about 2085 cm^{-1} can be used to monitor the changes in the electron density in the cluster core upon population of the excited state.

After irradiation into the lowest-energy absorption band of cluster $\mathbf{1}^{2+}$, the TRIR spectra at early time delays (<3 ps) display instantaneous bleaching of the parent ν(CO) bands together with the appearance of broad transient absorptions due to the excited state of $\mathbf{1}^{2+}$. As for the reference cluster $[Os_3(CO)_{10}(^i$Pr-AcPy)] (Figure 6a), the highest-frequency band of $\mathbf{1}^{2+}$ at 2088 cm^{-1} shifts to larger wavenumbers by ca. 11 cm^{-1} in the excited state. In fact, at $t_d = 1$ ps (Figure 6b), two broad transient absorption bands are observed on the high-frequency side of the 2088 cm^{-1} bleach at 2099 and 2121 cm^{-1}, respectively. Within less than 10 ps, the transient absorption bands in the terminal ν(CO) region sharpen up and slightly shift (by ca. 6 cm^{-1}) to higher frequency. These spectral changes are attributed to early relaxation processes (vibrational cooling and solvation).[43−47] On the same time scale, the 2121 cm^{-1} band further develops at the expense of the 2099 cm^{-1} band, being gradually shifted to 2127 cm^{-1} and reaching its maximum intensity at ca. 10 ps. On a longer time scale (up to 500 ps), the 2127 cm^{-1} band also decays while the parent cluster largely recovers. The position of the 2099 cm^{-1} band, shifted to larger wavenumbers by ca. 11 cm^{-1} with respect to the highest-frequency ground-state band, is in good agreement with that of the highest-frequency transient ν(CO) band at 2093 cm^{-1} in the TRIR spectrum of $[Os_3(CO)_{10}(^i$Pr-AcPy)] at $t_d = 3$ ps (Figure 6a). The 2099 cm^{-1} band is therefore assigned to $\mathbf{1}^{2+}$ in its $\sigma\pi^*$ excited state, the shift to larger wavenumbers resulting from a decreased π-back-donation to the carbonyl ligands due to depopulation of a σ(Os−Os) bonding orbital. Upon decay of the 2099 cm^{-1} band, the ν(CO) band at 2121 cm^{-1} further develops and shifts to larger wavenumbers by ca. 40 cm^{-1} relative to the highest-frequency ground-state band. This large shift is consistent with formal one-electron oxidation of the cluster core. Indeed, similar IR spectral changes are observed upon electrochemical oxidation of the related clusters $[Os_3(CO)_{10}(\alpha$-diimine)] (vide infra).

In line with the photooxidation of the cluster core, the transient 2121/2127 cm^{-1} band is ascribed to $\mathbf{1}^{2+}$ in a charge-separated (CS) excited state where an electron has been transferred from the cluster core to the remote viologen unit. As the latter band grows in at the expense of the 2099 cm^{-1} band, the TRIR spectra clearly prove that the population of the CS excited state takes place via a fast decay of the initial $\sigma\pi^*$ state. This observation corresponds with the ps TA spectra of $\mathbf{1}^{2+}$ (vide supra). The relatively small shift (11 cm^{-1}) of the ν(CO) bands in the $\sigma\pi^*$ excited state compared to the value for the CS state (40 cm^{-1}) can be explained by the electron-donating capacity of the temporarily reduced α-diimine ligand, partly compensating for the electron deficiency at the triosmium core. In the CS state, the electron residing on the α-diimine moiety has been transferred to the remote viologen acceptor site, leaving the cluster core formally one-electron-oxidized. Importantly, the TRIR data also prove that there is hardly any direct nonradiative decay

(43) Owrutsky, J. C.; Baronavski, A. P. *J. Chem. Phys.* **1996**, *105*, 9864−9873.
(44) Yang, H.; Snee, P. T.; Kotz, K. T.; Payne, C. K.; Harris, C. B. *J. Am. Chem. Soc.* **2001**, *123*, 4204−4210.
(45) Dougherty, T. P.; Heilweil, E. J. *J. Chem. Phys.* **1994**, *100*, 4006−4009.
(46) Dougherty, T. P.; Heilweil, E. J. *Chem. Phys. Lett.* **1994**, *227*, 19−25.
(47) Liard, D. J.; Busby, M.; Matousek, P.; Towrie, M.; Vlček, A., Jr. *J. Phys. Chem. A* **2004**, *108*, 2363−2369.

from the relaxed $\sigma\pi^*$ excited state to the ground state, which would compete with the electron transfer. This is inferred from the observation that the ground-state bleach at 2038 cm^{-1} only shows a minor decrease in signal intensity within the first 5 ps after excitation. This behavior is in contrast with the nonradiative decay of 40% of [Os$_3$(CO)$_{10}$(^{i}Pr-AcPy)] molecules in the $\sigma\pi^*$ state to the ground state (vide supra), demonstrating the efficiency of the subsequent electron transfer to the viologen moiety.

To get more insight into the kinetics of the CS state, the well-separated transient ν(CO) band at 2121 cm^{-1} was selected for Gaussian curve fitting. The same procedure was repeated with the 2099 cm^{-1} band characterizing the $\sigma\pi^*$ excited state, even though with a limited precision due to the low intensity of this band. Spectral fitting, while fixing the width of these two bands, enabled us to determine the peak areas. From the dependence of the peak area of the 2121 cm^{-1} band on the time delay, both the rise time (2.1 ± 0.2 ps) and lifetime (75 ± 10 ps) of the CS state have been derived. The rise time of the CS state compares well with the decay time of the 2099 cm^{-1} band. The $\sigma\pi^*$ excited-state lifetime $\tau = 2.1$ ps in acetone was used to determine the forward electron-transfer rate constant k_f according to eq 1, where $\tau_{ref} = 17 \pm 2$ ps is the $\sigma\pi^*$ excited-state lifetime of the reference cluster [Os$_3$(CO)$_{10}$(^{i}Pr-AcPy)] under the same experimental conditions.

The resulting value $k_f = 4.2 \times 10^{11}$ s^{-1} is in good agreement with the lower limit of 4×10^{11} s^{-1} derived from the ps TA experiments (vide supra). The lifetime of the CS excited state also compares reasonably well with the result obtained from the TA measurements.

$$k_f = 1/\tau - 1/\tau_{ref} \quad (1)$$

Nanosecond Transient Absorption Spectra of the Dyad [Os$_3$(CO)$_{10}$(AcPy-MV)]$^{2+}$ (1^{2+}). Excitation into the lowest-energy transition of the reference cluster [Os$_3$(CO)$_{10}$(^{i}Pr-AcPy)] in non- or weakly coordinating solvents (2-chlorobutane, toluene, THF, acetone) results in homolytic splitting of an Os−Os(α-diimine) bond and concomitant formation of open-structure biradicals [$^{\bullet}$Os(CO)$_4$−Os(CO)$_4$−$^{+}$Os(Sv)(CO)$_2$(α-diimine$^{\bullet-}$)] (Sv = solvent). To find out if similar biradical photoproducts are formed from the relaxed $\sigma\pi^*$ excited state of cluster **1**$^{2+}$, nanosecond transient absorption (ns TA) spectra of the latter cluster were recorded in acetone. The ns TA spectra were obtained by irradiating cluster **1**$^{2+}$ by the 550 nm line of a tunable Coherent Infinity XPO laser and monitoring spectral changes in the wavelength region 350−800 nm. The TA spectra recorded directly after the laser pulse reveal a weak bleaching between 430 and 615 nm due to disappearance of **1**$^{2+}$ and very weak transient absorptions below 430 nm and in the long wavelength region. On longer time scales (up to 1.5 μs) the transient species almost completely converts back to the parent cluster **1**$^{2+}$. As the ns TA spectra of **1**$^{2+}$ closely resemble those of [Os$_3$(CO)$_{10}$(^{i}Pr-AcPy)] in acetone,[40] the observed transient absorptions are accordingly assigned to the open-structure biradical [$^{\bullet}$Os(CO)$_4$−Os(CO)$_4$−$^{+}$Os(Sv)(CO)$_2$(AcPy$^{\bullet-}$−(CH$_2$)$_2$−MV^{2+})](PF$_6$)$_2$ (Sv = acetone). On the basis of a comparison between the ΔA values observed for **1**$^{2+}$ and those obtained after irradiation of an isoabsorptive solution of [Os$_3$(CO)$_{10}$(^{i}Pr-AcPy)], the amount of biradicals formed from the $\sigma\pi^*$ excited state of **1**$^{2+}$ is reduced by approximately 80%. Assuming similar molar absorbances for both biradicals, the quantum yield for the biradical formation out of **1**$^{2+}$ is calculated, using the value for [Os$_3$(CO)$_{10}$(^{i}Pr-AcPy)] in acetone (0.6, as estimated from the ps TRIR spectra), to be approximately 12%. The latter value is in excellent agreement with the observed shortening of the $\sigma\pi^*$ excited-state lifetime from 17 ps for [Os$_3$(CO)$_{10}$(^{i}Pr-AcPy)] to 2.1 ps for **1**$^{2+}$ in this solvent. On the basis of this result, we conclude that approximately 88% of the molecules decay rapidly to the lower-lying CS state.

Scheme 5. Qualitative Excited-State Potential Energy Curves and Photoreactivity of Cluster **1**$^{2+}$ in Acetone

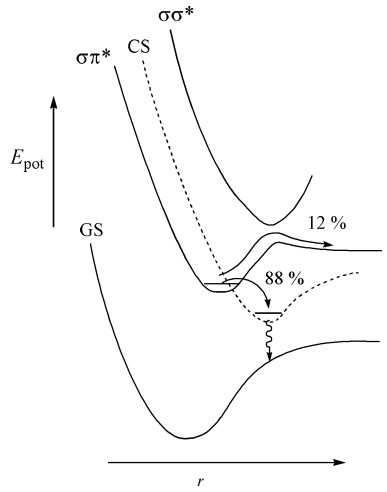

The decay processes for the optically excited cluster **1**$^{2+}$ in acetone are depicted in terms of the qualitative potential energy curves in Scheme 5. In agreement with the results of the TRIR experiments, irradiation into the lowest-energy absorption band of **1**$^{2+}$ leads to the population of a $\sigma\pi^*$ excited state, in which one electron has been transferred from the cluster core to the lowest π^*(α-diimine) orbital. From this excited state, a minor part (12%) of the cluster molecules produces biradicals detectable in the residual TA and TRIR spectra (t_d = 500 ps), whereas the major part (88%) undergoes fast decay to the charge-separated (CS) state.

Photochemistry of the Dyad [Os$_3$(CO)$_{10}$(AcPy-MV)]$^{2+}$ (1^{2+}) in Coordinating Acetonitrile. Nanosecond TA spectra of cluster **1**$^{2+}$ were also recorded in coordinating MeCN. Contrary to the situation in acetone, the TA spectra obtained in MeCN did not indicate the presence of solvent-stabilized biradicals. Instead, strong bleaching was observed between 400 and 600 nm due to the disappearance of **1**$^{2+}$. In addition, fairly intense transient absorption bands arose at 390 nm and at about 630 nm, already within the laser pulse. These transient features closely resemble those observed in the TA spectra of **1**$^{2+}$ in acetone on the picosecond time scale and are accordingly attributed to the absorption of the methyl viologen radical cation (MV$^{\bullet+}$). This assignment implies that irradiation of **1**$^{2+}$ in MeCN results in electron transfer from

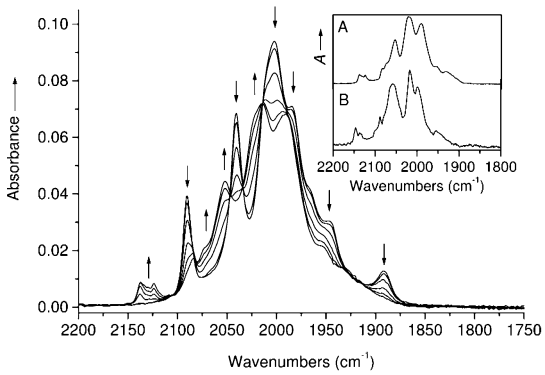

Figure 7. IR spectral changes accompanying photolysis of cluster $\mathbf{1}^{2+}$ in MeCN at 293 K (λ_{irr} = 514.5 nm). Inset: IR spectra obtained upon (A) photooxidation of $\mathbf{1}^{2+}$ and (B) electrochemical oxidation of $[Os_3(CO)_{10}(^{i}Pr\text{-}AcPy)]$ in a thin-layer electrochemical cell.

the cluster core to the viologen moiety, producing the relatively long-lived CS state. On longer time scales (up to 1 ms), however, no regeneration of the parent cluster was observed, the intensity of the absorption bands attributed to the $MV^{\bullet+}$ moiety even having increased. As the latter spectral changes most likely reflect accumulation of a long-lived photoproduct, continuous-wave (CW) irradiation experiments were performed to get more insight into the nature of the latter species.

Upon continuous-wave irradiation with the 514.5 nm line of an argon-ion laser, the solution of cluster $\mathbf{1}^{2+}$ in MeCN turned blue (due to the $MV^{\bullet+}$ absorption). The photogenerated species showed IR ν(CO) bands at 2137 (w), 2123 (w), 2083 (w), 2071 (sh), 2053 (m), 2020 (vs), 1990 (s), 1956 (w), and 1932 (w) cm^{-1} (see Figure 7). It is noteworthy that the photoproduct is fairly stable at room temperature and could be formed in relatively high yields (up to 85%). The shift of the ν(CO) bands to much larger wavenumbers compared with parent cluster $\mathbf{1}^{2+}$ points to significantly decreased π-back-bonding toward the carbonyl ligands and is consistent with the formal one-electron photooxidation of the cluster core. In fact, the above ν(CO) pattern (Figure 7, inset A) closely resembles that obtained separately by irreversible electrochemical oxidation of the reference cluster $[Os_3(CO)_{10}(^{i}Pr\text{-}AcPy)]$ in MeCN ($E_{p,a}$ = +0.16 V vs Fc/Fc^+) (Figure 7, inset B). Although research is in progress to assign the oxidation product(s), a preliminary spectroelectrochemical study of a series of clusters $[Os_3(CO)_{10}(\alpha\text{-diimine})]$ revealed that the shift of the ν(CO) bands to larger wavenumbers upon oxidation is dependent on the α-diimine ligand used. [In fact, the MeCN solution after the oxidation contains a mixture of at least two different species, the ratio being dependent on the coordinating solvent and the oxidation method applied (bulk electrolysis, thin-layer electrolysis, chemical oxidation, etc.).] Notably, reverse reduction of the oxidation product(s) of $[Os_3(CO)_{10}(^{i}Pr\text{-}AcPy)]$ in MeCN results in nearly complete regeneration of the parent cluster. These results indicate that, upon oxidation, the clusters $[Os_3(CO)_{10}(\alpha\text{-diimine})]$ undergo a reversible structural change, with the α-diimine coordination being retained.

On the basis of the results of the continuous-wave irradiation and the observed transient bands characteristic for $MV^{\bullet+}$ in the ns TA spectra of $\mathbf{1}^{2+}$ in MeCN, the blue-colored photoproduct is proposed to result from an electron-transfer reaction similar to that observed in acetone, one electron being again transferred from the cluster core to the viologen moiety. However, differently from the CS state of $\mathbf{1}^{2+}$ in acetone, the photoproduct in MeCN does not regenerate the parent cluster, even on the time scale of minutes. This behavior clearly reflects the influence of the solvent: in contrast to acetone, the MeCN molecules coordinate strong enough to prevent the back electron transfer, inducing a secondary thermal reaction of the photooxidized cluster core in the "locked" CS state.

Table 1. Electrochemical Data for Cluster $\mathbf{1}^{2+}$ and Its Reduction Products[a]

cluster[b]	$E_{1/2}$ (V)	ΔE_p (mV)[c]	$E_{p,a}$ (V)
$\mathbf{1}^{2+}$	−0.77	90 (80)	+0.15 (irr)
$\mathbf{1}^{\bullet+}$	−1.18	90 (80)	
1	−1.61	100 (80)	
$\mathbf{1}^{\bullet-}$	−1.92 (irr)[d]		

[a] Conditions and definitions: 10^{-3} mol dm^{-3} solutions in MeCN (containing 10^{-1} M Bu_4NPF_6) at 293 K; Pt disk microelectrode; υ = 100 mV s^{-1}; redox potentials vs $E_{1/2}$ (Fc/Fc^+); ΔE_p, peak-to-peak separation for a redox couple; $E_{p,a}$, anodic peak potential for oxidation of cluster $\mathbf{1}^{2+}$; chemical irreversibility denoted by irr. [b] Assignments given in the main text. [c] ΔE_p for the Fc/Fc^+ internal standard in parentheses. [d] $E_{p,c}$, cathodic peak potential for reduction of cluster $\mathbf{1}^{\bullet-}$.

Table 2. IR ν(CO) Wavenumbers of Cluster $\mathbf{1}^{2+}$ and Its Reduction Products[a]

cluster[b]	ν(CO) (cm^{-1})
$\mathbf{1}^{2+}$	2089 (m), 2040 (s), 2002 (vs), 1986 (s, sh), 1964 (sh), 1948 (sh), 1893 (w)
$\mathbf{1}^{\bullet+}$	2087 (m), 2038 (s), 1999 (vs), 1984 (s, sh), 1962 (sh), 1898 (w)
1	2085 (m), 2036 (s), 1998 (vs), 1981 (s, sh), 1959 (sh), 1898 (w)
$\mathbf{1}^{\bullet-}$	2050 (mw), 2011 (m), 1972 (vs), 1952 (s, sh), 1863 (w)

[a] Conditions: 5×10^{-3} mol dm^{-3} solutions in MeCN (containing 10^{-1} M Bu_4NPF_6) at 293 K; in situ reduction within an IR OTTLE cell.[36] [b] Assignments given in the main text.

Electrochemistry of the Dyad $[Os_3(CO)_{10}(AcPy\text{-}MV)]^{2+}$ ($\mathbf{1}^{2+}$). Cyclic voltammetric and IR/UV−vis spectroelectrochemical studies of the cluster $[Os_3(CO)_{10}(AcPy\text{-}MV)]^{2+}$ ($\mathbf{1}^{2+}$) were performed to identify the reduction steps and to investigate whether the electron-trapping function of the viologen moiety may be switched reversibly by an external potential bias. The redox potentials of cluster $\mathbf{1}^{2+}$ and its reduction products are presented in Table 1, and the corresponding ν(CO) wavenumbers are collected in Table 2.

The cyclic voltammogram of $\mathbf{1}^{2+}$ in MeCN shows at room temperature two fully reversible cathodic waves at $E_{1/2}$ = −0.76 V and −1.17 V vs Fc/Fc^+ (peaks R_1 and R_2 in Figure 8) together with a nearly reversible third cathodic step at $E_{1/2}$ = −1.60 V (peak R_3). In accordance with the results of the IR and UV−vis spectroelectrochemical experiments (vide infra) and the redox potentials reported for related viologen-linked α-diimine systems,[25−28,42] the first two cathodic steps represent consecutive one-electron reductions of the viologen unit, producing radical cation $\mathbf{1}^{\bullet+}$ and neutral cluster **1**. Further reduction of **1** at the potential $E(R_3)$ yields the corresponding radical anion $\mathbf{1}^{\bullet-}$. The unpaired electron in $\mathbf{1}^{\bullet-}$ is most likely localized on the α-diimine ligand, consistent with the comparable reduction potentials of the

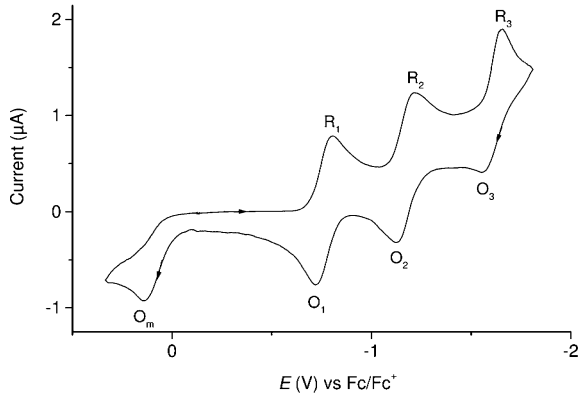

Figure 8. Cyclic voltammogram of cluster $\mathbf{1}^{2+}$ at $T = 293$ K. Conditions: 10^{-3} M cluster in MeCN/10^{-1} M Bu_4NPF_6; Pt disk microelectrode (0.42 mm^2 apparent surface area); $v = 100$ mV s^{-1}.

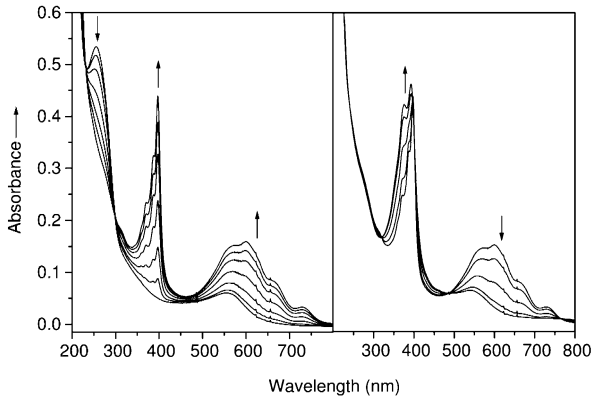

Figure 9. UV−vis spectral changes accompanying the first (left) and second (right) one-electron reduction step of cluster $\mathbf{1}^{2+}$ in MeCN at 293 K.

reference clusters [$Os_3(CO)_{10}$(^{i}Pr-PyCa)] (^{i}Pr-PyCa = σ-*N*,σ-*N*′-pyridine-2-carbaldehyde-*N*-isopropylimine) ($E_{1/2} = -1.69$ V vs Fc/Fc^+)[31] and [$Os_3(CO)_{10}$(^{i}Pr-AcPy)] ($E_{1/2} = -1.76$ V vs Fc/Fc^+).

The first two reduction steps of cluster $\mathbf{1}^{2+}$ were conveniently followed in situ by UV−vis spectroscopy, using an OTTLE cell (Figure 9). Exhaustive electrolysis at −0.76 V in MeCN resulted in the appearance of the characteristic bands[41] of the methyl viologen radical cation ($MV^{\bullet+}$) at 398 nm and around 600 nm. At the same time, the absorption band of MV^{2+} at 256 nm disappeared. During the subsequent reduction of $\mathbf{1}^{\bullet+}$, the intense band at 398 nm slightly shifted to higher energy while its high-frequency shoulder at 376 nm increased significantly in intensity. The broad absorption band of $\mathbf{1}^{\bullet+}$ around 600 nm disappeared, leaving behind a less intense absorption band at 543 nm. The UV−vis spectral changes accompanying the second reduction step are in good agreement with the one-electron reduction of the $MV^{\bullet+}$ moiety to neutral MV.[41] As free MV itself does not absorb above 500 nm,[41] the absorption band of **1** at 543 nm is attributed to a transition having a predominant cluster core-to-π*(AcPy) character. The corresponding lowest-energy absorption band of nonreduced cluster $\mathbf{1}^{2+}$ lies at a slightly lower energy, viz. at 558 nm (Figure 9).

IR spectroelectrochemistry also proves that the first two cathodic steps occur at the remote viologen unit. In particular,

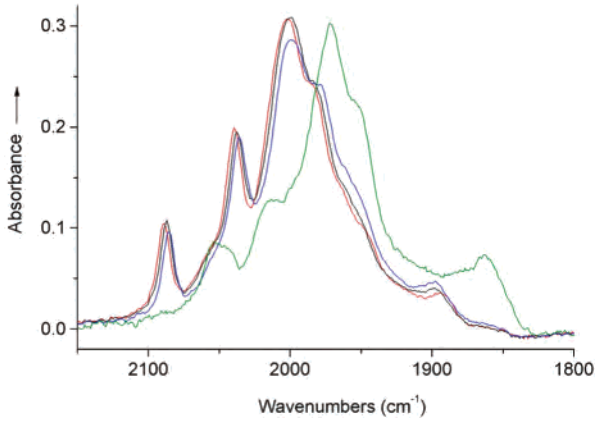

Figure 10. IR spectra of $\mathbf{1}^{2+}$ (red) and the series of its one-electron reduction products $\mathbf{1}^{\bullet+}$ (black), **1** (blue), and $\mathbf{1}^{\bullet-}$ (green) in MeCN at 293 K. Note that the spectrum of $\mathbf{1}^{\bullet-}$ is a difference spectrum.

stepwise reduction of $\mathbf{1}^{2+}$ at room temperature produces radical cation $\mathbf{1}^{\bullet+}$ and neutral cluster **1** with nearly identical IR ν(CO) patterns, the bands being shifted to lower frequency by merely 2 and 4 cm^{-1}, respectively, compared to the parent cluster (Figure 10). On the other hand, a previous study has shown that formation of radical anions [$Os_3(CO)_{10}$(α-diimine)]$^{\bullet-}$ (α-diimine = e.g., 2,2′-bipyrimidine), with the added electron largely localized on the α-diimine ligand, results in a much larger ν(CO) shift of ca. 15 cm^{-1} to smaller wavenumbers compared with the parent clusters.[48] Rapid reduction of **1** (within 1 min) in the OTTLE cell allowed spectroscopic detection of radical anion $\mathbf{1}^{\bullet-}$ that has a ν(CO) pattern nearly identical with that of **1**, the ν(CO) bands being however shifted by ca. 25−30 cm^{-1} to smaller wavenumbers (Table 2). This shift confirms that the third added electron in $\mathbf{1}^{\bullet-}$ is localized on the α-diimine ligand. The thermal stability of radical anion $\mathbf{1}^{\bullet-}$ at room temperature is, however, limited; it reacts further before the reduction of parent cluster **1** is completed. Radical anion $\mathbf{1}^{\bullet-}$ is nevertheless considerably more stable than its analogues [$Os_3(CO)_{10}$(^{i}Pr-PyCa)]$^{\bullet-}$ and [$Os_3(CO)_{10}$(^{i}Pr-AcPy)]$^{\bullet-}$ that live merely seconds at fairly low temperatures.[31]

Photochemistry of One-Electron-Reduced [$Os_3(CO)_{10}$(AcPy-$MV^{\bullet+}$)] ($\mathbf{1}^{\bullet+}$). The results of the combined cyclic voltammetric and IR/UV−vis spectroelectrochemical studies of cluster $\mathbf{1}^{2+}$ clearly prove that the first two reduction steps for $\mathbf{1}^{2+}$ are localized on the viologen unit. As already the first one-electron reduction of MV^{2+} significantly reduces its electron-accepting character, we investigated in the next step whether the photochemical behavior of $\mathbf{1}^{2+}$ could be controlled by an externally applied electronic bias. To properly address the effect of this external stimulus and to prove whether the characteristic photochemistry of the ordinary [$Os_3(CO)_{10}$(α-diimine)] clusters can be restored, the photoreactions of cluster $\mathbf{1}^{\bullet+}$ (with the viologen moiety one-electron-reduced prior to photoexcitation) were studied in acetone at 240 K and in coordinating MeCN at room temperature. Under the selected experimental conditions, the clusters [$Os_3(CO)_{10}$(α-diimine)] form solvent-stabilized zwitterions that regenerate the parent cluster on a time scale of

(48) van Outersterp, J. W. M. Ph.D. Thesis, University of Amsterdam, 1995.

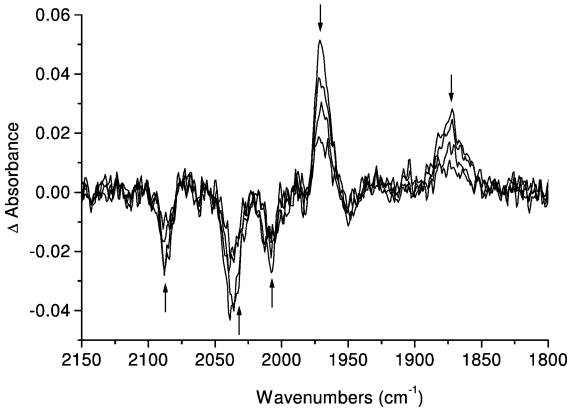

Figure 11. Difference-absorption rapid scan IR spectra of one-electron-reduced cluster $\mathbf{1}^{\bullet+}$ in MeCN, measured at time delays of 1, 2, 4, and 6 s after the 488 nm laser excitation.

seconds or shorter (Scheme 4). In line with this behavior, CW irradiation of $\mathbf{1}^{\bullet+}$ in acetone and MeCN did not induce any significant photochemical conversion. To decide whether the negligible photoreactivity was caused by the inertness of the populated excited state or by a rapid and complete back reaction of transients to the parent cluster, the photoreactions of $\mathbf{1}^{\bullet+}$ were followed with rapid-scan FTIR spectroscopy in the (sub)second time domain. After the complete one-electron reduction of $\mathbf{1}^{2+}$ in an OTTLE cell, the product $\mathbf{1}^{\bullet+}$ was irradiated for 4 s by an argon-ion laser (488 nm, 300 mW) and the following IR spectral changes in the CO-stretching region were monitored on the time scale of seconds to minutes. The difference IR spectra of $\mathbf{1}^{\bullet+}$ in MeCN, measured 0−6 s after the laser pulse, are depicted in Figure 11. The difference-absorption IR spectra recorded directly after the photoexcitation of $\mathbf{1}^{\bullet+}$ in acetone (240 K) and MeCN display instantaneous bleaching of the parent ν-(CO) bands (negative signals) together with two transient bands at 1970 (s) and 1873 (m, br) cm^{-1}. The observed transient absorption bands closely resemble those observed upon irradiation of $[Os_3(CO)_{10}(^{i}Pr\text{-}AcPy)]$ in MeCN (compare Figures 3c and 11) and are accordingly ascribed to the solvent-stabilized zwitterion $[^{-}Os(CO)_4-Os(CO)_4-^{+}Os(Sv)(CO)_2(AcPy\text{-}MV^{\bullet+})]$ (Sv = acetone, MeCN). Both the transient absorptions and parent bleaches decay due to complete regeneration of the parent cluster. As the spectra recorded in MeCN were of higher quality than those obtained in acetone, the lifetime of the solvent-stabilized zwitterion ($\tau \sim 6$ s) could only be determined in the former, more strongly coordinating solvent.

The formation of zwitterions upon irradiation of $\mathbf{1}^{\bullet+}$ is indicative of a greatly diminished driving force for the oxidative quenching of the $\sigma\pi^*$ excited state by the reduced viologen moiety. In contrast to the results for $\mathbf{1}^{2+}$, the photoinduced electron transfer to the latter unit is therefore no longer feasible. Instead, one-electron reduction of the viologen unit restores the "original" photochemical behavior observed[40] for the reference cluster $[Os_3(CO)_{10}(^{i}Pr\text{-}AcPy)]$. The lifetime of the zwitterion formed upon irradiation of $\mathbf{1}^{\bullet+}$ (6 s) is, however, significantly reduced compared to that of its nonsubstituted derivative lacking the electron-accepting moiety (38 s).[29] This difference cannot be explained by electronic reasons, as $[Os_3(CO)_{10}(\alpha\text{-diimine})]$ clusters form longer-lived zwitterions when using more electron-accepting α-diimines (2,2′-bipyrimidine, $\tau = 9.0$ s in MeCN, vs 2,2′-bipyridine, $\tau = 5.6$ s in MeCN).[29] In the case of $\mathbf{1}^{\bullet+}$, the reduced zwitterion lifetime is tentatively ascribed to a Coulombic destabilization of the zwitterion by the cationic viologen moiety ($MV^{\bullet+}$). Alternatively, previous photoisomerization studies of this type of clusters have shown that the position of the chelating α-diimine ligand may change concomitantly with the Os−Os bond cleavage producing the zwitterion.[30] Steric hindrance of the MeCN coordination caused by the movement of the AcPy ligand with the viologen sidearm may also contribute to the shorter zwitterion lifetime.

Most importantly, the rapid-scan IR results have shown that the photochemical behavior of $\mathbf{1}^{2+}$ changes upon the one-electron reduction of the viologen unit and, indeed, can be controlled by an external potential bias. Similar control of the photochemical or photophysical behavior by reduction of a remote electron-acceptor unit has been reported for $\{Ru(bpy)_3^{2+}-\text{electron acceptor}\}$ dyads bearing reversibly reducible viologen[42] or *p*-quinone units.[49] For example, the quenching of the emitting ^{3}MLCT excited state of a $\{Ru(bpy)_3^{2+}-MV^{2+}\}$ dyad, where the viologen moiety is covalently attached to the 4-position of one of the bipyridine ligands, changes its nature from oxidative to reductive upon the one-electron reduction of the MV^{2+} unit.[42]

In summary of the redox-controlled photochemistry of $\mathbf{1}^{2+}$ in coordinating media (Scheme 6), irradiation of the reduced form ($\mathbf{1}^{\bullet+}$) results in splitting of an Os−Os(α-diimine) bond and ultimate formation of solvent-stabilized open-structure zwitterions detectable by rapid scan FTIR spectroscopy. As the structural change upon the zwitterion formation is completely reversible, the read-out of the reduced state is nondestructive. Upon irradiation of the oxidized form ($\mathbf{1}^{2+}$) rapid electron transfer to the remote viologen site is observed, resulting in photooxidation of the cluster core. Notably, the latter process shows close correspondence with the irreversible electrochemical oxidation of $[Os_3(CO)_{10}(^{i}Pr\text{-}AcPy)]$. While in acetone this electron-transfer process results in the formation of a short-lived CS state that almost completely regenerates the parent cluster, irradiation of $\mathbf{1}^{2+}$ in MeCN gives rise to the formation of a long-lived charge-separated photoproduct that does not thermally regenerate $\mathbf{1}^{2+}$.

Conclusions

Transient absorption and time-resolved IR spectroscopies on the picosecond time scale document that irradiation of cluster $\mathbf{1}^{2+}$ in coordinating solvents induces an ultrafast electron transfer from the cluster core to the remote viologen moiety. This process results either in a short-lived CS state (acetone) or in a stable charge-separated photoproduct (acetonitrile), depending on the coordinating ability of the solvent. The occurrence of the electron transfer and the

(49) Goulle, V.; Harriman, A.; Lehn, J.-M. *J. Chem. Soc., Chem. Commun.* **1993**, 1034−1036.

Scheme 6. Redox-Controlled Photochemistry of Cluster $\mathbf{1}^{2+}$ in Coordinating Media

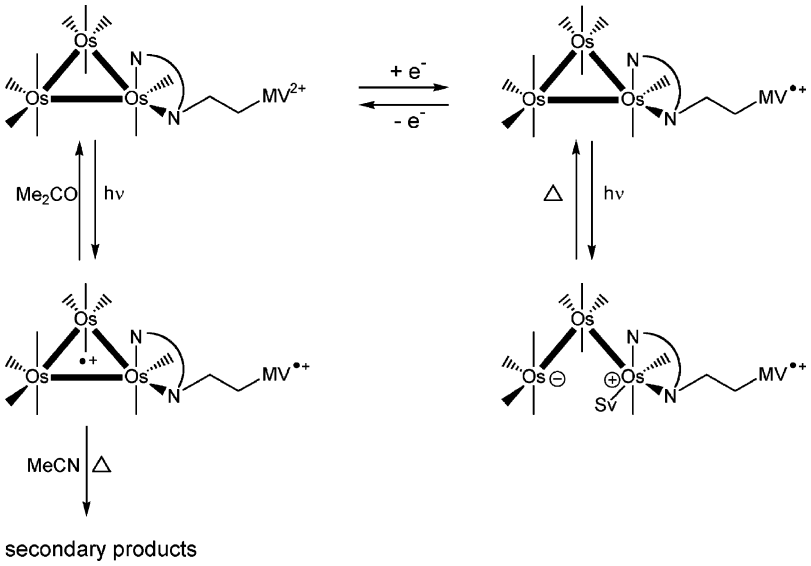

concomitant structural change upon light excitation can be controlled by the redox state of the viologen moiety. Electrochemical one-electron reduction of the viologen unit lowers its electron-accepting ability to such an extent that the photoinduced electron transfer to the latter unit is no longer feasible. Instead, irradiation of reduced $\mathbf{1}^{\bullet+}$ results in the formation of zwitterions, the common photoproducts for the clusters [$Os_3(CO)_{10}$(α-diimine)] in strongly coordinating solvents.

In general, the thorough understanding of the photochemical behavior of the reference cluster [$Os_3(CO)_{10}$(^{i}Pr-AcPy)] has allowed us to design the [$Os_3(CO)_{10}$(α-diimine-MV)]$^{2+}$ (donor−acceptor) dyad where the photoreactivity can be controlled electrochemically by changing the oxidation state of the MV unit. However, as the MV unit is actively involved in the cluster photochemistry, the system cannot be regarded as a molecular redox switch.

In extension of this research, the involvement of transition metal clusters in (supra)molecular systems capable of signal generation and selective transfer is not only challenging but may also find important applications in the field of molecular nanoelectronics. It is also noteworthy that the observed selective one-electron photooxidation of the cluster core may provide interesting novel activation pathways, thereby opening a new and stimulating research area in the field of cluster chemistry (catalysis).

Acknowledgment. Financial support has been received from the Council for Chemical Sciences of the Netherlands Organization for Scientific Research (CW-NWO, Project No. 348-032; F.W.V. and F.H.) and from the European Union (LSF ref. No. USEV13C2/01). We also thank the reviewers of this article for their valuable comments.

IC049191N